Environment-Induced Electrostatic Discharges as the Cause of Voyager 1 Power-On Resets

P. Leung,* A. C. Whittlesey,* H. B. Garrett,† and P. A. Robinson Jr.‡
Jet Propulsion Laboratory, California Institute of Technology, Pasadena, California

The Pioneer and Voyager spacecraft all experienced anomalous behavior during their encounters with Jupiter. In particular, the Voyager 1 spacecraft experienced 42 electrical upsets in the electrical circuitry designed to protect the on-board computer from power fluctuations. Given the diversity of instrumentation and frequency of the anomalies observed by Voyager 1 in the inner magnetosphere of Jupiter, this set of data is particularly well suited as a case study. Although the nature of the anomalies clearly indicates a spacecraft-charging origin, the Voyager low-energy plasma data apparently imply absolute surface potentials of only a few tens of volts. It is thus difficult to explain the anomalies in terms of surface charging. The anomalies are, however, shown to be consistent with the hypothesis of internal charging of spacecraft parts and components.

Nomenclature

EMI = electromagnetic interference
ERT = Earth-received time
ESD = electrostatic discharge
FDS = flight data subsystem
HGA = high-gain antenna
IESD = internal electrostatic discharge
LECP = low-energy charge particles
LGA = low-gain antenna
PLS = plasma science
POR = power-on reset
PPS = photopolarimeter
PRA = planetary radio astronomy
PWS = plasma wave subsystem
R_J = Jupiter radius
RTG = radioisotope thermoelectric generator

Introduction

AMONG the most exciting events of the space age have been the Pioneer and Voyager encounters with the outer planets. Whereas the near-flawless performance of these vehicles has generally been known and appreciated, there has been little discussion of the anomalous behavior of the vehicles. Of the two missions, the Voyager vehicles had the more complete complement of instrumentation for studying plasma interactions. Further, these vehicles were carefully designed to avoid the worst aspects of spacecraft charging—a primary cause of anomalies. Even so, Voyager 1 experienced 42 anomalies in the inner Jovian magnetosphere. The purpose of this paper will be to review the facts surrounding these anomalies and to attempt to explain their cause. Although it will not be possible to explain them unambiguously, the results point strongly to internal charging and discharging of parts and components internal to the outer surface of the spacecraft as the possible agent.

In the first part of this paper, the Voyager spacecraft and instrumentation will be described. Following this, Jupiter's environment will be discussed. Next, the anomalies and the results of efforts at reproducing them will be presented. As these results imply the existence of an arcing source, the rest of the paper will concentrate on possible mechanisms for generating an arc.

The Voyager Mission

The Voyager spacecraft were launched on August 20 (Voyager 2) and September 5, 1977 (Voyager 1). The objective of the Voyager mission has been to conduct exploratory investigations of Jupiter, Saturn, the interplanetary medium, and, if possible, Uranus and Neptune. Voyager 1 encountered Jupiter on March 5, 1979, passing within 4.5 R_J (Jupiter radius = R_J = 71,400 km). Voyager 2 passed within 10.1 R_J on July 9, 1979.

A schematic diagram of the Voyager 1 spacecraft is presented in Fig. 1. As shown, the vehicle consists of a main frame, a 3.66-m-diam high-gain disk antenna, a science boom, and three radioisotope thermoelectric generators (RTGs). (Additional details may be found in Refs. 1 and 2.) To reduce the effects of spacecraft charging on Voyager, an extensive electrostatic control program was undertaken.[3] For example, to make the spacecraft an equipotential surface, the thermal blankets covering the spacecraft body, normally a dielectric

Table 1 Exposed dielectrics.

External dielectrics	Application
Kapton thermal blankets	Several
Teflon thermal blankets	Numerous
External cabling jacketing	Numerous
Teflon	Especially magnetometer boom
Other dielectrics	Numerous small segments
Sunshapes—Kapton with VDA	Over thermal blanket apertures
White paint (PV-100)	High-gain antenna (HGA)
White paint (PV-100)	Thermal control on spacecraft bus
Black paint	Antenna support structures
Optics	Science instruments and Startracker
Connector socket rubber matrix	Separation connectors
RTG oxide coating	Thermal radiator
Teflon/silver radiator	IRIS instrument detector heat sink
Brewster plate	PPS calibration target
Kapton tape	Edge of HGA
Kapton tape	Miscellaneous locations
Radome	RF feed horn cover
Miscellaneous	Cable clamps, brackets
Fiberglass struts	Magnetometer boom
Fiberglass struts	Science instrument supports
Dacron cloth tape	Magnetometer boom extension restraint

Received Sept. 29, 1981; revision received Oct. 25, 1985.

*Member of Technical Staff, Reliability Engineering Section. Member AIAA.
†Group Supervisor, Reliability Engineering Section. Member AIAA.
‡Staff Scientist, Reliability Engineering Section. Member AIAA.

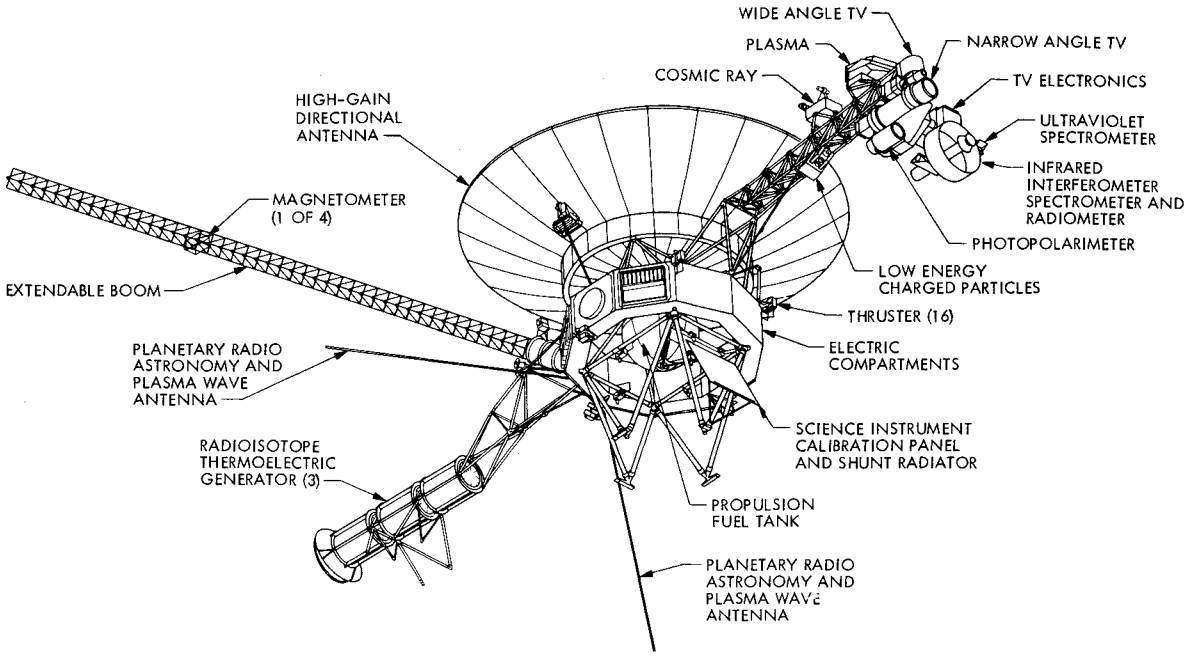

Fig. 1 Schematic diagram of the deployed Voyager showing the various science instruments.

Table 2 Estimates of ESD voltages at PRA/PWS antenna terminals

Source	Thickness, cm	Area, cm^2	C_x, pf[a]	C_f, pf[b]	t_r, ns[c]	tp, ns[d]	$V_{Breakdown}$, kV	V_{ANT}, V^e	V_{PRA}, mV[f]
Antenna collar: Arc to antenna	0.32	10.13	5.64	0.96	3	100	1	40.7	1.16
Antenna collar: Arc across collar	0.32	10.13	5.64	0.96	3	100	1	7.12	0.203
Antenna tip Kapton: Arc to space	0.005	1.27	44	0.353	3	50	4	952	6.80
Antenna tip Kapton: Arc across Kapton	0.005	1.27	44	0.353	3	50	4	12.4	0.087
Brewster plate	0.005	560	20,000	12	3	325	1	0.84	0.253
Frequency selective subreflector (FSS)	27	4750	19.4	21.6	8	588	7	1.78	1.78

[a]Capacitance across the sample. [b]Capacitance to spacecraft. [c]Rise time of the discharge pulse. [d]Pulse width of the discharge pulse. [e]Voltage across the antenna. [f]Voltage at the input of PRA.

surface, were covered with a black conductive paint. Despite this careful charge-control program, numerous dielectrics still exist on the satellite surface (Table 1). These are typically either small in area or limited in their charging. For example, the surface of the high-gain antenna is covered with paint, PV-100. The properties of this paint were determined by electron irradiation tests[4] to behave like a leaky dielectric and not to change more negative than -1700 V under any circumstances.

Despite the careful precautions taken with Voyager, voltages caused by electrostatic discharge (ESD) at the input of the planetary radio astronomy (PRA) were predicted early in the mission[5] (see Table 2). These subsystems were believed to be the most sensitive on the spacecraft and the most likely to record transients, if they existed. Unfortunately, the PRA and plasma-wave subsystem (PWS) best-viewing modes (from an ESD-monitoring standpoint) were only a small portion of the total observation time during the key Jupiter encounter period and, as will be shown, did not provide any definite evidence.

These calculations, based on known and extrapolated plasma characteristics, indicated that Voyager 1 would have ESDs within 25 R_J and especially within 8 R_J (Voyager 1's closest approach was 4.9 R_J). Estimated times to charge materials up to discharge potentials ranged from 700 s or more to less than 46 s when the spacecrat was close to Jupiter. Finally, since photoemission is considered a dominant charge-neutralization mechanism, it was expected that the solar occultation would allow the whole spacecraft to charge to some negative but uniform value. In this state, no significant potential differences across the surface that would cause ESDs were expected. As will be discussed, the actual charging results differed considerably from these predictions. Even so, the 8-to-4 R_J region did turn out to be the most active from an anomalies standpoint.

Scientific Instruments

The science boom provides a mounting for the science scan platform and, inboard of the platform, the Low-Energy Charge Particles (LECP) experiment, the cosmic ray instruments, and the plasma science experiments (PLS). The PLS instrument and the dipole antenna, which are shared by the PWS and the PRA experiments, provide the most valuable plasma data for this study. It should also be noted that a Brewster plate, which is a thick dielectric, is part of the scientific package and is a likely source of arcs.

The PLS instrument provided data on the low-energy plasma environment between 10 and 5950 eV. The instrument consists of four standard modulated grid Faraday cups. By choosing the proper operating modes, the density temperature and composition of the Jovian plasma environment can be determined.[1,2]

The plasma data for charged particles with energies greater than 14 keV are provided by the LECP instrument. The solid-state detectors of this instrument can detect electrons between 14 keV and 10 MeV and ions between 30 keV and 150 MeV. The detectors have a wide dynamic range and good energy resolution.[2] The resolvable energy range of the LECP instrument does not overlap with that of the PLS instrument, however. This results in a void in plasma data energy between 6 and 14 keV for the electrons and 6 and 30 keV for the ions.

The PWS instrument provides data on the electromagnetic and electrostatic signals between 10 Hz and 56 kHz. It is a balanced electric dipole antenna with a 2-m effective length. The PWS experiment has, as predicted, proven to be a valuable data source for the ESD investigation. In the normal format it operates in a 16-channel spectrum analyzer mode (10 Hz to 56 kHz); each channel has a bandwidth of 10% of its center frequency. For brief periods of time, the PWS operates in a wideband waveform mode (10 Hz to 12 kHz) that yields a time, frequency, and amplitude display.[2] The wideband waveform mode with its 28 kHz bandwidth offers an opportunity to observe the radiated electromagnetic interference (EMI) directly as a spike in the frequency time diagram. The PRA instrument, which shares the same antenna with the PWS instrument, provides the measurement of frequency spectra in the range of 1.2 to 40 MHz. Both the PWS and the PRA instruments give measurements of the local plasma frequency. Since the plasma density is proportional to the plasma frequency, these two instruments provide independent measurements of the local plasma densities.

Jupiter's Magnetosphere and Distribution of Charged Particles

Low-Energy Particles

Both Voyager 1 and Voyager 2 provided extensive environmental information from their encounters with Jupiter. In the following, however, we will emphasize the trajectory of Voyager 1. Voyager 1 crossed the bow shock of Jupiter on February 28, 1979 (day 59) and was within Jupiter's magnetosphere until March 22 (day 80), with the closest approach of 4.5 R_J coming at noon on March 5, 1979. During this period, various instruments, described earlier, provided detailed measurements of the field and particle properties of the magnetosphere. These data will be reviewed below.

Figure 2a is the trajectory of Voyager 1, projected onto the orbital plane of Jupiter, with the x-axis pointing toward the sun and with the center of Jupiter as the origin. Figure 2b, a drawing of the magnetosphere, is derived from the plasma wave and magnetometer experiments on board both Voyagers.

The magnetosphere[6,7] extends about 60 R_J from Jupiter on the dayside and about 160 R_J in that portion of the predawn quadrant traversed by Voyagers 1 and 2. At its boundaries, some features of Jupiter's magnetosphere (e.g., a boundary layer, magnetosheath, and tail) resemble those of the Earth's magnetosphere. Deep inside, however, the magnetosphere is dominated by two unique features, namely, fast rotation, which produces significant centrifugal forces on the charged particles, and a strong source of heavy ions from the satellite Io. These result in a persistent torus of plasma near Io's orbit at 6 R_J with plasma densities up to 3000 cm^{-3}.

Associated with each region of the Jovian magnetosphere are different distributions of charged particles. Factors affecting these plasma distributions are the plasma sources and the magnetic field. The strong magnetic field lines of Jupiter tend to contain the charged particles and cause them to corotate with the field lines, consequently imparting an azimuthal velocity to the plasma. As Jupiter has a very high angular

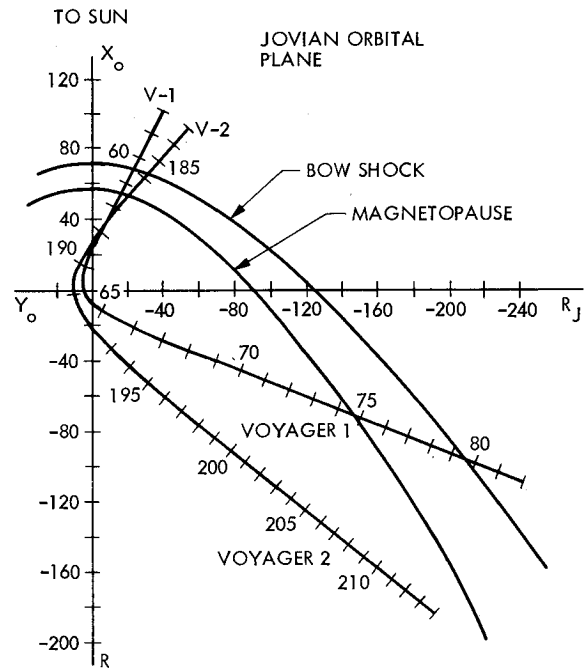

Fig. 2a Trajectory of the Voyager spacecraft.

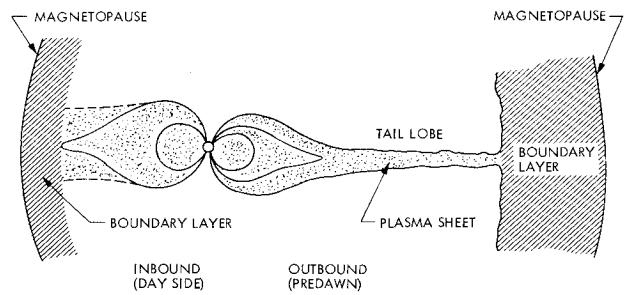

Fig. 2b Jupiter's magnetosphere.

velocity (period = 10 h), the corotation velocity can be as high as 250 km at a distance of 20 R_J. The electrons have a thermal velocity much higher than the corotation velocity and thus are not significantly affected by corotation; whereas the ions within the magnetosphere usually have a temperature of less than 100 eV (thermal velocity = 25 km/s) and are dominated by corotation. Because of its strong dipole moment, the theoretical limit (Alfven limit) for corotation is determined to be about 40 R_J.[8] Experimentally, the PLS instrument aboard Voyagers 1 and 2 found that the azimuthal flow velocity[9] of low-energy ions followed the corotation value up to 20 R_J, beyond that the measured value is below the predicted value. The LECP instrument, however, reported that rigid corotation was observed to a distance of 60 R_J. In any case, the ions have an azimuthal velocity whose value in the torus region is less than the corotation velocity. Typical ion spectra are shown in Fig. 3, along with the spatial plasma density profile. Notice that the plasma density is very high ($n > 100/cm^3$) around the torus region.

Table 3 summarizes the plasma parameters[10] that were observed in different regions of the Jovian magnetosphere. The data were mainly derived from the PLS instrument on board Voyagers 1 and 2. The LECP instrument provided the data for ions of energy greater than 15 keV. The electron distributions are characterized by two components, a cold and hot component, and are tabulated in Table 3. The source of cold electrons is believed to be Io, where they are produced by the impact ionization of neutral molecules ejected by Io. The hot electrons may have their origin in the mid-latitude region of the outer magnetosphere. The transport of electrons from

Table 3 Plasma paramters of Jupiter's magnetosphere

			Outer magnetosphere		Middle magnetosphere	Io torus	
	Magnetosheath	Boundary layer	Mid-lat	Plasma sheet	Plasma sheet	Warm	Cold
Density of cold electrons, cm^{-3}	1	—	—	0.1	1.5	1900	1900
Temperature of cold electrons, eV	50	—	—	30	20	5	5
Density of hot electrons, cm^{-3}	0.01	0.01	0.001	0.01	0.1	3	3
Temp. of hot electrons, eV	1000	1000	3000	3000	3000	1000	1000
Density of ions, cm^{-3}	1.01	0.01	0.001	0.11	1.6	1903	1903
Temperature of ions, eV	1000	1000	30,000	100	40	28	1
Effective ion mass number, AMU	1	1	1	1	14	14	14
Corotation velocity, km/s	250	250	200	200	120	65	50
Spacecraft potential, V	−1	−1	−1	−1	−7	−14	−16
Upper limit of the potential of the Brewster plate V_{bph}, V	−4	−7	−2	−23	−166	−15	−17
Lower limit of the potential of the Brewster plate V_{bpl}, V	−4	−7	−2	−24	−190	−25	−467

Photocurrent density = 0.025 nA/cm^2.

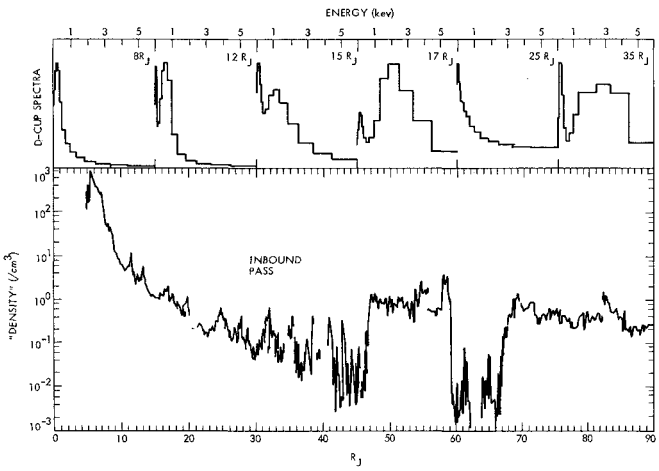

Fig. 3 Ion spectra at various distances from Jupiter (top); ion density as a function of distance from Jupiter (bottom).

one region to another is achieved by cross-field diffusion of magnetic flux tubes via classical and non-classical processes. The cold electrons are the dominant species around the Io torus and the inner magnetosphere. The hot electrons are the dominant species in the outer magnetosphere—the average temperature of electrons increases steadily from inner to outer magnetosphere.

Ion composition plays an important role in the Jovian magnetosphere. As the neutral molecules injected by volcanic eruptions on Io are in the form of sulphur dioxide, the dominant ion species in the Io torus and the inner magnetosphere are oxygen and sulphur. Protons from the solar wind become the dominant species in the outer magnetosphere. The ion temperature in the torus is relatively low (1 eV) and the ion temperature in the outer magnetosphee is very high (20 keV). The ion temperature decreases steadily from the outer magnetosphere to the inner magnetosphere.

High-Energy Particles

Besides the cold electrons just discussed, another population of electrons with energy $E \geq 40$ keV is also present in the Jovian magnetosphere. These particles are trapped by the dipole magnetic field of Jupiter and undergo three periodic motions: gyration about the local magnetic field line, latitudinal bounce between mirror points along the field line, and longitudinal drift with respect to the corotation field lines. The first gyration motion for particles with magnetic moments in the range 100 to 2000 MeV/Gauss also generates synchotron radiation and is detected on Earth as decimeter radiation (3000 MHz). The lifetime of these energetic electrons is approximately one year. Figure 4 displays the flux of radiation electrons for $E \geq 1.5$ MeV along the Voyager trajectory. The electron flux increases as the planet is approached, peaking in the vicinity of the Io torus. The radiation electron flux at Jupiter is very intense and is about two orders of magnitude higher than that of Earth's environment. Also shown in Fig. 4 is the total plasma density determined by the PRA instrument.

Since high-energy electrons are able to penetrate the shielding of the spacecraft, they can cause damage to the electronic systems of the spacecraft. Consequently, a precise knowledge of the radiation environment is very important for the survival of Jupiter-bound spacecraft. As a result, a model of the radiation environment has been developed and was used as a design guideline on Voyagers 1 and 2 for protecting the vital parts of the spacecraft from radiation damage. Figure 5 is a typical energy spectrum of radiation electrons obtained from the model at a distance of 4.5 R_J. The role that these high-energy electrons may have in spacecraft charging will be discussed in subsequent sections.

Voyager 1 Power-On Resets at Jupiter

The Voyager 1 spacecraft experienced numerous anomalous events during the Jupiter flyby, most of which were subsequently determined to be related to 42 power-on resets (POR) within the Flight Data Subsystem (FDS). The PORs are believed to have been caused by ESD events as described in the following paragraphs.

The Voyager FDS is an on-board computer system containing a volatile memory system. It was feared that power-line undervoltage transients could cause malfunctions of the memory and computer operations with no warning of the malfunctions. To avoid the problem, a POR system is incorporated in the FDS as shown in Fig. 6a. The key element is the undervoltage sensor that continually monitors the power supply voltage. If an undervoltage occurs, the sensor sends a digital signal to the delay logic electronics which stop processing, stop the internal clock, reinitialize the computations as needed, wait a period of time, and restart computer activity if the undervoltage condition has ceased. The minimum period of time lost is about 175 ms. These 175-ms outages can be identified by gaps in the data stream and by 175-ms discrepancies in the timing of spacecraft activities. A list of the 42 PORs, two suspect PORs, and their Earth-received times (ERTs, Greenwich Mean Time) are shown in Table 4.

Spacecraft data analysis showed that the POR event occurred spatially as indicated in Fig. 4. The timing of these PORs suggests a charging origin, as they occurred with greater frequency as the spacecraft went deeper into the Jupiter plasma environment, as earlier predicted, and disappeared during the sun occultation. To validate this hypothesis, the POR circuit was tested for its sensitivity to electrical transients. It was found that the PORs were not initiated by the circuit which normally triggers the logic buffer, the 10-V logic undervoltage

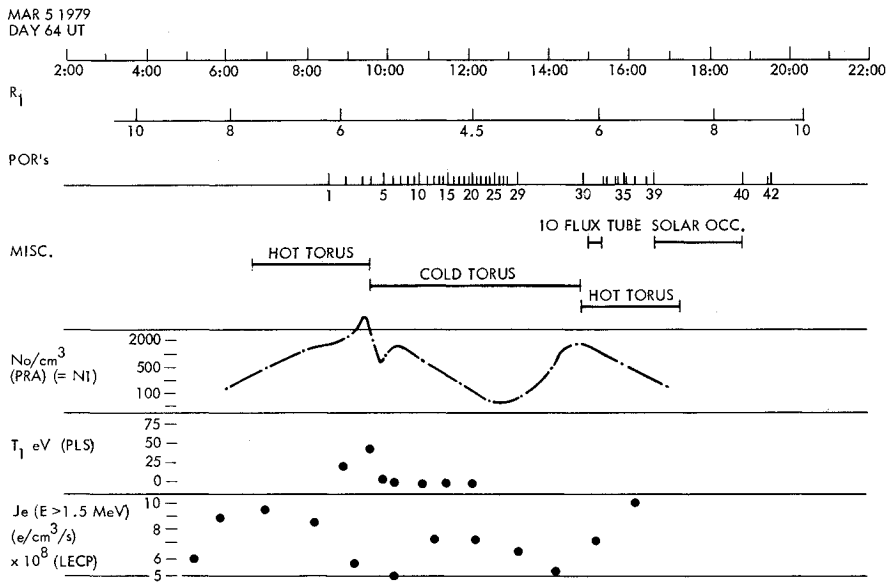

Fig. 4 Timeline showing the PORs and various plasma parameters.

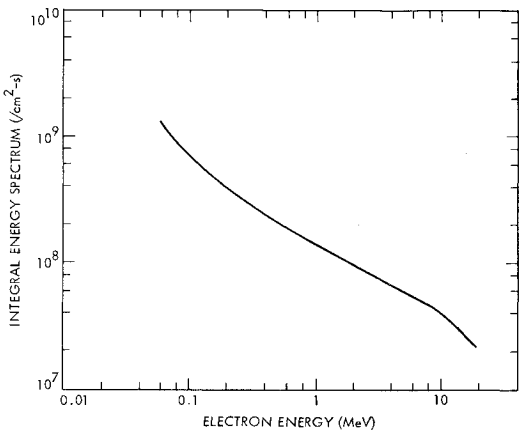

Fig. 5 High energy electron spectra at 4.5 R_J.

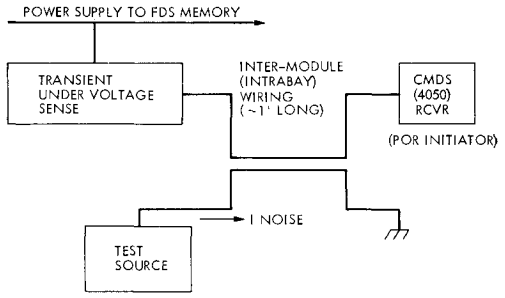

Fig. 6a ESD test on POR circuitry.

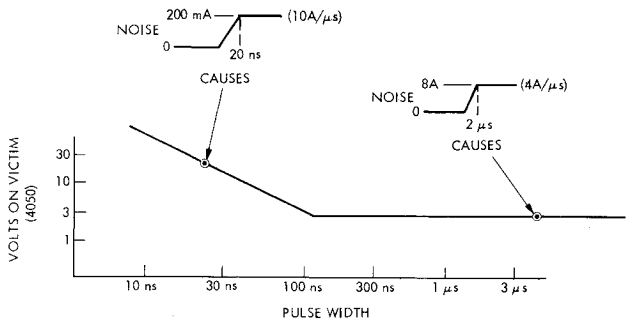

Fig. 6b Pulse parameter required to cause PORs.

sensor in the 2006A1 module, because the 2006A1 module would have reset the Ultraviolet Subsystem (UVS) high voltage and FDS memory logic, neither of which occurred. The sensitive element was not the power-line undervoltage sensor, but the CD4050 input buffer in the processor delay logic circuitry (module 2006A5). This is located in an electronic circuit board about 8 in. away from the undervoltage sense circuitry. The interconnecting wiring is routed in common with other system wiring and, as indicated in Fig. 7, it is possible that ESD noise currents were carried by another wire into the spacecraft and passed near the POR interconnecting wiring. To test this hypothesis, an experiment was performed as shown in Fig. 6a. A 200-mA pulse of a current with a risetime of 20 ns in the adjacent 2-ft wire caused a 17-V, 20-ns pulse on the processor delay logic and triggered the circuit. An 8-A 2-μs current pulse caused a 3-V, 5-μs voltage pulse on the processor delay logic warning and triggered the circuit (Fig. 6b). The current pulse slopes are 10 and 4 A/μs, respectively (that is, the rates are roughly comparable). These results are compatible with the charging hypothesis.

Differential Charging of Spacecraft Surfaces

Electrostatic discharge[11] (ESD) has been considered as a cause of electronic anomalies in many Earth-synchronous satellites. Discharges typically occur when the voltage stress across materials or between surfaces exceeds their breakdown voltage. The voltage stress occurs in response to the complex interactions of electrons and ions with spacecraft surfaces (external and internal), which results in a net accumulation of charge on the spacecraft. Since different surfaces are subjected to different charging rates (some are sunlit and some are not, and secondary emissions differ), it is possible that some surfaces will acquire the high-voltage stress necessary to create an ESD. A way to cure this problem is to make all surfaces conductive or grounded to each other. Most spacecraft, however, including Voyager, have some dielectric surfaces such as thermal control surfaces, calibration targets, and optics. As already discussed, the Voyager project was concerned that the near-Jupiter plasma environment might cause ESDs and took numerous precautions. Even so, it was unable to make a completely ESD-secure spacecraft. As a result, ESDs are a real possibility on Voyager and, as described, might generate the PORs. This possibility will be discussed in the following.

In order to evaluate the range of potentials to be expected in the Jovian environment, a simple model[12] was developed to estimate the satellite-to-space potential. The satellite is as-

Table 4 Voyager 1- Jupiter encounter time/significant events March 5 (day 64), 1979

Event	Time UTC, h:m:s	Time relative, h:m:s	Time relative, decimal hours
Closest approach	12:04:35.4	0:00:00	0.00
FDS anomalies			
POR 1	8:27:07	−3:37:28	−3.62
2	8:55:57	−3:08:38	−3.14
3	9:19:41	−2:44:44	−2.75
4	9:37:48	−2:23:46	−2.23
5	9:50:49	−2:13:46	−2.23
6	10:05:56	−1:58:39	−1.98
7	10:17:09	−1:47:26	−1.79
8	10:27:32	−1:37:03	−1.62
9	10:38:37	−1:25:58	−1.43
10	10:47:56	−1:16:39	−1.28
11	10:58:17	−1:06:18	−1.11
12	11:05:44	−:58:51	−0.98
13	11:15:12	−:49:23	−0.82
14	11:21:41	−:42:54	−0.72
15	11:28:50	−:35:45	−0.60
16	11:36:32	−:28:03	−0.47
17	11:44:35	−:20:00	−0.33
18	11:52:32	−:12:03	−0.20
19	11:59:26	−:05:09	−0.09
20	12:04:42	−:00:11	−0.003
21	12:09:57	+:05:26	+0.09
22	12:16:19	:11:44	0.20
23	12:24:01	:19:26	0.32
24	12:31:33	:26:58	0.45
25	12:36:21	:31:46	0.53
26	12:44:45	:40:10	0.67
27	12:51:53	:47:18	0.79
28	12:57:41	:53:06	0.89
29	13:07:40	1:03:05	1.05
30	14:52:19	2:47:44	2.80
31	15:22:16	3:17:41	3.29
32	15:23:52	3:19:17	3.32
33	15:38:52	3:34:17	3.57
34	15:45:06	3:40:32	3.68
35	15:51:17	3:46:42	3.78
36	15:52:29	3:47:54	3.80
37	16:04:41	4:00:06	4.00
38	16:13:29	4:08:54	4.15
39	16:18:17	4:13:42	4.23
40	18:48:28	6:43:53	6.73
41	19:13:28	7:08:53	7.15
42	19:32:17	7:27:42	7.46

sumed to be a conducting sphere. In equilibrium the currents to its surface balance:

$$I_E - (I_I + I_{SE} + I_{SI} + I_{BSE} + I_{PH}) = 0 \qquad (1)$$

where I_E is the incident electron current, I_I the incident ion current, I_{SE} the secondary electrons due to electron impact, I_{SI} the secondary electrons due to ion impact, I_{BSE} the backscattered electrons due to electron impact, and I_{PH} the photoelectron emission current.

The electron current is given by

$$I_E = 4\pi r_s^2 \cdot \frac{{}_qN_{EO}}{2} \frac{{}_2T_E{}^{1/2}}{\pi M_e} e(-V/T_E) \quad (V<0) \qquad (2)$$

and for the ions:

$$I_I = \pi r_s^2 \cdot {}_qN_{Io} v_s \qquad (V<0) \qquad (3)$$

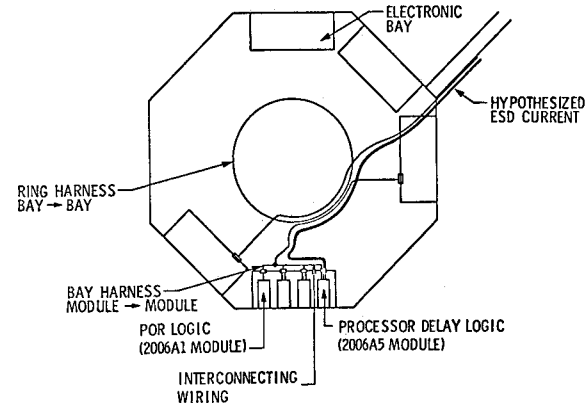

Fig. 7 POR circuit wiring in Voyager spacecraft.

where r_s is the satellite radius, q the unit charge, N_{EO} the ambient electron density, N_{Io} the ambient ion density, V the satellite potential, v_s the satellite velocity relative to ions, T_E the ambient electron temperature, and M_e the electron mass.

In Eqs. 2 and 3, the ion current is assumed to be dominated by the corotation velocity of the plasma, v_s (see earlier), and thus only intercepts the cross-section of the vehicle. Positive potentials were considered, but according to the computations, only negative potentials were found. Parametric expressions were assumed for I_{SE}, I_{SI}, I_{BSE}, and I_{PH} in terms of T_E and T_I. (T_I was assumed to be $\frac{1}{2} Mv_s^2$). V was then varied until Eq. (1) was found to hold.

The potentials computed according to the model are listed in Table 3 for various Jovian regimes and for illuminated or shadowed surfaces. As would be anticipated from the low electron temperatures, no potentials in excess of −100 V were found. Similar computations in which the photoelectron flux was ignored or in which the sheath was assumed to be "thick" or "thin" gave comparable results. These results are collaborated by the in-situ measurements. Scudder et al.[13] claim the satellite potential never exceeded −40 V and in fact was normally a few volts positive. Similar results were reported by McNutt et al.[14] for the positive ion data. It appears, therefore, from both the experimental and theoretical data, that the Voyager 1 spacecraft could never have exceeded −1100 V during the POR events. These voltages are well below the −5000 V normally believed to be required for arcing.

These calculations of the surface potential differ significantly from the previous FDS predictions. In these calculations, the plasma environment was derived from Voyager 1 data, whereas in Ref. 5 a hypothetical environment was used. The hypothetical environment neglected the following facts: 1) the plasma in the inner magnetosphere was very dense, and 2) the number of cold electrons within the torus region was relatively large. Consequently the previously predicted spacecraft potentials had large negative values and were very dependent on the presence of sunlight.

Although the satellite-to-space potential is below the breakdown potential normally associated with arcing, the possibility that an isolated dielectric surface may have charged to a higher potential due to flux and isotropies or other "exotic" processes remains. To estimate the potential on an isolated dielectric, a leakage current has to be included in the current balance equation (Eq. 1). Since the leakage current depends on the equivalent resistance of the dielectric surface area, the resultant potential will depend on the resistivity of the dielectric material. The exposed dielectric surfaces on Voyager 1 have small areas compared to the total conducting area of the spacecraft. Therefore, the ion current collected by the dielectric surfaces will depend critically on its orientation with respect to the direction of corotation. The collected ion current can range from the corotation ion current to the thermal ion current. In the last two rows of Table 1 the upper (V_{bph}) and lower (V_{bpl}) limits of the surface voltage on a

typical exposed dielectric material, the Brewster plate, are displayed. The Brewster plate is chosen for the sample calculation because it is made of dielectric material of high resistivity ($\rho = 10^{17}$ Ω-cm) and thus is very susceptible to ESD, due to surface charging. From Table 3, the maximum differential potential at the Brewster plate at the region where PORs occurred is 450 V, which occurred within the hot torus. The thickness of the Brewster plate is 2 mm; hence, the maximum electric field inside the Brewster plate is only 2250 V/cm, which is well below the breakdown value of 10^6 V/cm for most dielectric materials.

From the above analysis, it appears that surface charging of the spacecraft, although it cannot be completely ruled out, is an unlikely cause of an ESD event and thus cannot account for the occurrence of PORs. One of the problems encountered in the surface potential calculations is, however, the limited amount of data available. Further, because the PLS detectors were oriented in the wrong direction during the outbound journey there were few ion data after the closest approach. Thus we cannot perform any detailed analysis to explain the gaps in which no PORs occurred (from 13:07 to 14:52 and during sun occultation). Even so, it is unlikely that new data would significantly alter the conclusion that surface charging is low during the PORs.

Thruster Firings

When the thrusters of the attitude-control circuits are fired, the residual ionization products in the effluent can short-circuit any potential differences that have developed across the spacecraft surface and may result in an artificial discharge. The times of attitude-control thruster firings were examined to see if a) they might be the cause of EMI, or b) they might act as a trigger for an ESD/POR event. Of 39 thruster firings examined in the critical time period, 16 appeared to be near a POR. Although well over half of the coincidental POR/thruster firings were with yaw thrusters, this is explained by the greater frequency of yaw-thruster firings rather than a POR/yaw-thruster cause-effect relationship. Further, examination of the POR data shows a uniform rate trend which would become more non-uniform if those PORs coincidental with thruster firings were removed. It is concluded that there appears to be no cause-effect relationship between thruster firings and the PORs.

Spacecraft Modes

The spacecraft operating modes were examined to see if internal activity could have directly caused PORs or if internal activity caused enhanced susceptibility to ESDs and created new noise-coupling paths. One observed correlation was the photopolarimeter (PPS). It had an electrical fault in its polarizer filter wheel (see Fig. 1 timing diagram) at 6:00 more than two hours before the first POR; it was turned off at 13:07, coincing with the stopping of PORs at 13:07 for 1 h and 45 min. The PORs restarted again, however, while the PPS was still off, thus showing that the PPS was at least not a principal cause of PORs. Another correlation is that the spacecraft attitude-control system went into the "all-axis inertial" mode at 13:11, after which there is a 1-hr 41-min gap with no PORs. Again, the PORs restarted at 14:52 without any corresponding spacecraft mode change. There appears to be no real connection between PORs and spacecraft modes.

Spacecraft Orientations

The spacecraft orientation was examined to see if it could have caused the 1¾ h gap in PORs. The hypothesis is that in sunlight, the spacecraft potential is near zero due to photemission, but a shadowed part may be charging and sparking. If that shadowed part were moved into sunlight, it would cease charging and sparking. The spacecraft was always referenced toward Earth and Canopus during the period of interest. Although the science-scan platform was continually being aimed at different targets, during the critical time period it showed no different orientation than when PORs were present.

"Exotic" Considerations

In the absence of a complete explanation, more exotic situations were considered, as follows:

1) Velocity/wake effects. It is possible that the source of sparking may not be a simple function of sunlit areas. Plasma corotation with Jupiter could create a wake and isotopics in the plasma flux. Local charging "hot spots" could occur. Similar processes at the Earth, however, have not been observed to result in significant potentials above the satellite-to-space potential.

2) Single-event upset. A penetrating particle causing a single-event upset is not suspected because, although this circuit element occurs throughout the spacecraft, only the circuit with the POR circuitry was effected.

Although these "exotic" sources cannot be ruled out, they require specialized conditions. Previous experience would tend to discount their importance.

Charge Deposition in Dielectrics

Another aspect of spacecraft charging is the deposition of charges by high-energy ($E > 40$ keV) electrons in the bulk dielectics and in ungrounded metallic parts located outside and inside the spacecraft structures. Charge deposition in the bulk of dielectric materials can create an electric field exceeding its dielectric strength, resulting in an ESD event. Charge deposition in ungrounded conductors can charge the conductors to a high potential. This potential may be high enough to break down the surrounding dielectric materials. Consequently, the energetic electrons can cause charging and discharging of spacecraft components not on the surface of the spacecraft. This phenomenon is called internal electrostatic discharge (IESD).

The integrated occurrences of PORs (Fig. 8) correlate with the fluence of electrons with energy greater than 10 MeV, making IESD a candidate for the PORs. Since electrons carry a much higher current and have a longer range than ions, the effect of ion flux is negligible in IESD. The average thickness of the Voyager spacecraft structure is 0.2 cm. This shielding will attenuate electrons with energy less than 1 MeV and reduce the flux of radiation electrons penetrating the spacecraft (Fig. 5) by an order of magnitude. Therefore, IESD has a higher probability of occurrence for materials and components located outside the structure of the spacecraft where the available shielding is minimal.

On Voyager 1, some cables were shielded from energetic electrons by thermal blankets only. The thermal blanket has an equivalent shielding thickness of 0.013 cm of aluminum. Consequently, the flux experienced by these cables is in the range of high 10^8 e/cm-s. After the Voyager's encounter with Jupiter, a test program was initiated to investigate the possibility of IESD for Jupiter-bound spacecraft. In one of the tests, cable bundles were tested. Cable bundles with Teflon and Kapton wire insulations were subjected to flux levels that Voyager 1 may have been exposed to at Jupiter. All the center conductors were connected to the ground plane through 50-Ω resistors. Discharges were observed to occur. The resulting transient signals were monitored on the center conductors of the tested cables. Figure 9 shows a typical signal monitored on a center conductor (50-Ω impedance). The peak voltage was about 0.8 V. In another test, several conductors in the cable bundle were left ungrounded. The observed transient characteristics were different from that of the grounded case. Figure 9b shows a typical signal observed during the discharge of the same cable bundle, but in the presence of floating conductors. The peak voltage approached 100 V and the pulse width was around 500 ns. It is suspected that the discharge first originated in the cable insulation, the plasma generated during the discharge then swept the extra charges stored in the

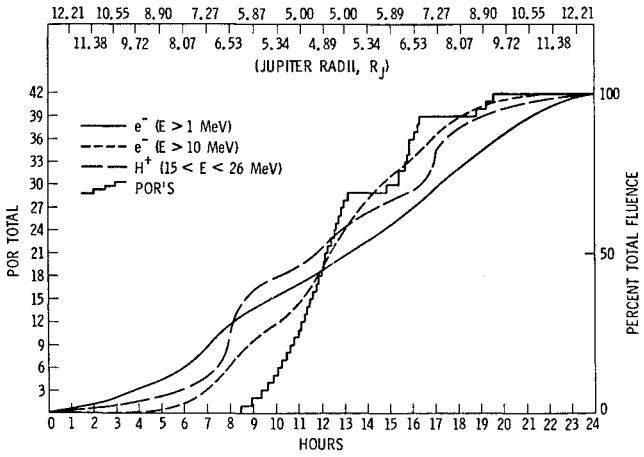

Fig. 8 Correlation of PORs with the high-energy electron fluence.

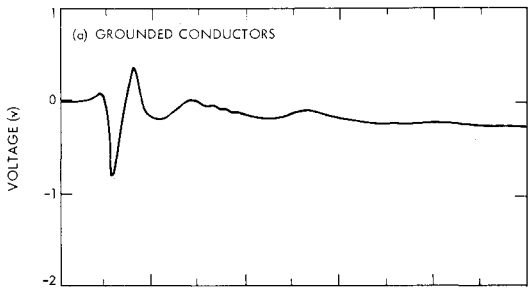

Fig. 9a Transient signals observed during a discharge of a Teflon cable bundle. All the conductors within the cable bundle were grounded.

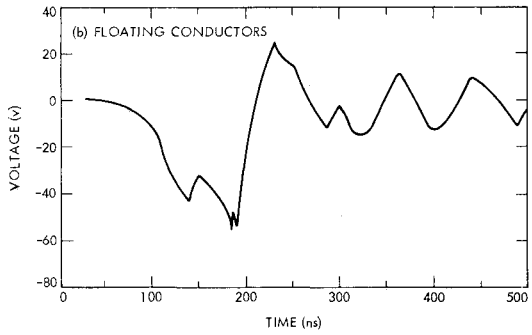

Fig. 9b Transient signals observed during a discharge of a Teflon cable bundle. Several conductors were floating during this test.

floating conductors, a discharge of large amplitude resulted, and a large signal was coupled to the grounded conductors (through the 50-Ω resistor). The signal displayed in Fig. 9b is certainly able to trigger a POR (Fig. 6). In the design of spacecraft cabling, it is customary to provide spare cables in a cable bundle. These spare cables are reserved for design changes. When these cables remain unused by launch time, the center conductors are usually left floating during the mission. It is very possible that floating conductors could have existed in the cable bundles of Voyager 1; consequently, the PORs may be triggered by the discharge of these floating conductors.

The above test results do not firmly imply that PORs are due to the discharging of cable bundles with floating conductors. To find the exact cause of PORs, the possibility of ESD in all external and internal dielectric materials and ungrounded conductors would have to be examined and the resultant coupling of the electromagnetic energy from the discharge pulse into the POR circuitry investigated. Even so, these discussions indicate that, whereas surface charging cannot adequately account for the POR event, internal charging can cause an ESD event. Thus IESD is the most likely candidate at this time for the occurrence of PORs in Voyager 1.

Correlation with PWS and PRA Data

Given that ESD did indeed trigger the PORs, the possibility exists that the transient electromagnetic signal generated by such arcs could be detected by the PWS antenna. The PWS data during encounter were investigated and, indeed, numerous spiky impulse-response functions such as would be associated with an arc were observed. Unfortunately, the PWS data intervals were limited and never corresponded with a POR occurrence. Further, the frequency of these events does not correlate with the frequency of PORs. Thus, although evidence does exist for ESDs, there is no conclusive evidence for or against ESDs in conjunction with the PORs. PRA data were very limited during the PORs regions. Although a possible event has been identified by the PRA, no possible PRA/ESD event coincided with a POR.

Conclusion

The Voyager satellites were carefully designed to prevent anomalous behavior due to charging and arcing. Even so, Voyager 1 experienced 42 anomalies. Electrostatic discharges (ESDs) have been demonstrated to be the probable cause of these anomalies. Several possible ESD sources were investigated. Although neither differential charging of spacecraft surfaces nor other "exotic" mechanisms cannot totally be ruled out, they are unlikely. Internal charging and the subsequent discharging appears to be a viable means of generating ESDs and, in turn, the power-on resets (PORs).

Acknowledgment

The research described in this paper was carried out by the Jet Propulsion Laboratory, California Institute of Technology, under contract with NASA.

References

[1]*Space Science Review,* 21, 1977.

[2]*Space Science Review,* 22, 1977.

[3]Whittlesey, A. C., "Voyager Electrostatic Discharge Program," *IEEE 1978 International Symposium on Electromagnetic Compatibility,* Atlanta, GA, 1978, p. 377-383.

[4]Stevens, J., NASA Lewis Research Center, private communication, 1978.

[5]Sanders, N., Inouye G., and Rosen, A., "Voyager Spacecraft Charging Immunization Support to JPL," TRW Report 31440-6002-RU-00, Redondo Beach, CA, 1977.

[6]Scarf, F. L., Gurnett, D. A., and Kurth, W. S., "Measurements of Plasma Wave Spectra in Jupiter's Magnetosphere," *Journal of Geophysical Research,* Vol. 86, 1981, pp. 8181-8198.

[7]Gurnett, D. A., Karth W. S., and Scarf, F. L., "The Structure of the Jovian Magnetotail from Plasma Wave Observation," University of California, Los Angeles, PPG-442, 1979.

[8]Kennel, C. F. and Coroniti, F. V., *Solar System Plasma Physics II,* edited by C.F. Kennel, L.J. Lanzerotti, and E.N. Parker, North-Holland, Amsterdam, 1979, p. 105.

[9]Bagenal F. and Sullivan, J.D., "Direct Plasma Measurements in the Io Torus and Inner Magnetosphere of Jupiter," *Journal of Geophysical Research,* Vol. 86, 1981, pp. 8447-8466.

[10]Divine, N. and Garrett, H. B., "Charge Particle Distributions in Jupiter's Magnetosphere," *Journal of Geophysical Research,* Vol. 88, 1983, pp. 6889-6993.

[11]Garrett, H. B., "The Charging of Spacecraft Surface," *Review of Geophysics and Space Physics,* Vol. 19, 1981, pp. 577-616.

[12]Tsipouras, P. and Garrett, H. B., "Spacecraft Charging Model—Two Maxwellian Approximations," AFGL-TR-79-0153, Air Force Geophysics Laboratory, Hanscom, MA.

[13]Scudder, J.D., Sittler, E.C., and Bridge, H.S., "A Survey of the Plasma Electron Environment of Jupiter: A View from Voyager," *Journal of Geophysical Research,* Vol. 86, 1981, pp. 8157-8180.

[14]McNutt, R. L. Jr., Belcher, J. W., and Bridge, H. S., "Positive Ion Observations in the Middle Magnetosphere of Jupiter," *Journal of Geophysical Research,* Vol. 86, 1981, pp. 8319-8342.